

Histone tails modulate nucleosome mobility and regulate ATP-dependent nucleosome sliding by NURF

Ali Hamiche[†], Ju-Gyeong Kang, Cynthia Dennis[†], Hua Xiao, and Carl Wu[‡]

Laboratory of Molecular Cell Biology, National Cancer Institute, National Institutes of Health, Building 37, Room 6068, Bethesda, MD 20892-4255

Edited by Gary Felsenfeld, National Institutes of Health, Bethesda, MD, and approved October 11, 2001 (received for review August 9, 2001)

Nucleosome Remodeling Factor (NURF) is an ATP-dependent nucleosome remodeling complex that alters chromatin structure by catalyzing nucleosome sliding, thereby exposing DNA sequences previously associated with nucleosomes. We systematically studied how the unstructured N-terminal residues of core histones (the N-terminal histone tails) influence nucleosome sliding. We used bacterially expressed *Drosophila* histones to reconstitute hybrid nucleosomes lacking one or more histone N-terminal tails. Unexpectedly, we found that removal of the N-terminal tail of histone H2B promoted uncatalyzed nucleosome sliding during native gel electrophoresis. Uncatalyzed nucleosome mobility was enhanced by additional removal of other histone tails but was not affected by hyperacetylation of core histones by p300. In addition, we found that the N-terminal tail of the histone H4 is specifically required for ATP-dependent catalysis of nucleosome sliding by NURF. Alanine scanning mutagenesis demonstrated that H4 residues 16-KRHR-19 are critical for the induction of nucleosome mobility, revealing a histone tail motif that regulates NURF activity. An exchange of histone tails between H4 and H3 impaired NURF-induced sliding of the mutant nucleosome, indicating that the location of the KRHR motif in relation to global nucleosome structure is functionally important. Our results provide functions for the N-terminal histone tails in regulating the mobility of nucleosomes.

The genome of eukaryotes is packaged into chromatin. The fundamental building block of chromatin is the nucleosome core particle, in which 147 bp of DNA is wrapped around a histone octamer in a left-handed superhelix (1). Chromatin structure plays a major role in processes such as transcription (2). Recent advances have revealed that chromatin structure is highly dynamic and subject to reversible changes in higher-order folding and nucleosome positioning (3, 4). These structural changes are largely mediated by enzymatic covalent modifications of the flexible N-terminal amino acids of the core histones and by noncovalent alterations of nucleosome architecture driven by ATP-dependent chromatin remodeling enzymes (3, 4).

Four classes of ATP-dependent chromatin remodeling complexes, each containing a member of the SWI2/SNF2 family of ATPases, have been characterized (4–8). Complexes containing SWI2/SNF2 or its highly related paralog STH1 (the SWI/SNF and RSC complexes) have been demonstrated to play a role in transcription (9–13). Complexes containing ISWI, Mi-2, and INO80 ATPases are also implicated in transcription and possibly other DNA transactions (14–18). Chromatin remodeling complexes that contain the ISWI ATPase include Nucleosome Remodeling Factor (NURF), ACF, CHRAC, RSF, WCRF, ISWI-B, and ISWI-D complexes in metazoans, and the Isw1 and Isw2 complexes in budding yeast (19–28). ISWI complexes remodel chromatin by mediating nucleosome “sliding,” the relative movement of a histone octamer *in cis*, without irretrievable displacement from DNA (29, 30). The actions of the SWI/SNF or RSC complexes allow greater disruption of nucleosome architecture. These complexes not only increase nucleosome mobility (8, 31) but also can create a stably remodeled nucleosome intermediate (32–34) and transfer a histone octamer from one DNA fragment to another (35).

Previous work from our laboratory has indicated that the nucleosome-stimulated ATPase activity of NURF is modulated by the flexible N-terminal histone tails (36). Removal of all N-terminal

histone tails from the nucleosome by trypsin digestion impaired the ATPase activity of NURF, suggesting that recognition of one or more histone tails by NURF is an important aspect of the remodeling mechanism (36). To investigate further the role of the N-terminal histone tails, we have characterized the effects of removing individual histone tails in reconstituted nucleosomes. We unexpectedly found that the histone tails, especially the histone H2B tail, can modulate the translational positioning of nucleosomes. In addition, we found that residues 16-KRHR-19 of the N-terminal histone H4 tail are critical for the ATP-dependent catalysis of nucleosome sliding by NURF.

Materials and Methods

DNA. The 359-bp *hsp70* (87A) fragment spans the promoter from positions –348 to +11 and originates from an *EcoRI* digest of plasmid pBSK359.3 m (29). The 256-bp fragment containing a sea urchin 5S RNA gene (37) was gel-purified from a *NciI* digest of plasmid pLV405–10 (38). The 357-bp fragment containing a sea urchin 5S RNA gene fused to the complete SP6 promoter was gel-purified from a *BamHI* digest of plasmid pB357 (39).

Histones. *Drosophila* histones were PCR amplified by using Vent-DNA polymerase from *Drosophila melanogaster* (Oregon R) genomic DNA. Histone globular domains were produced by removing the first 13 amino acids of H2A, the first 20 amino acids of H2B, the first 26 amino acids of H3, and the first 19 amino acids of H4. Wild-type (WT) histone H2B and H4 could not be expressed in *Escherichia coli*. Insertion of the ATA codon (Ile) immediately after the ATG dramatically increased their production to the same level as WT histones H2A and H3. We used PCR-directed mutagenesis to generate a series of mutations in the H4 N-terminal tail. Amino acids 9–11, 13–14, and 16–19 of H4 were substituted with alanines to generate H4 (9–11)A, H4 (13–14)A, and H4 (16–19)A. H3 and H4 N termini were exchanged by using PCR to create in-frame fusions of the first 20 amino acids of H4 and the first 27 amino acids of H3 to the globular domains of histone H3 and H4 (H4t-GH3 and H3t-GH4). Coding regions flanked by 5' *NdeI* and 3' *XhoI* sites were cloned in pET21b. PCR-generated insertions were cloned and sequenced for verification. BL21-CodonPlus-RIL (Stratagene) cells were routinely grown at 37°C on LB medium plus 0.1% glucose and selective pressure (ampicillin and chloramphenicol). Expression was induced at an A₆₀₀ of 0.6 by addition of isopropyl β-D-thiogalactoside to a final concentration of 1 mM, and the culture was incubated for 2 h at 37°C. Rifampicin (150 μg/ml) was added, and the culture was incubated for another 3 h. Cells were pelleted at 4,500 × g for 15 min. Individual histones were purified

This paper was submitted directly (Track II) to the PNAS office.

Abbreviations: WT, wild type; GST, glutathione S-transferase; NURF, Nucleosome Remodeling Factor.

[†]Present address: Laboratoire Biologie Moléculaire Eucaryote, Institut de Biochimie et Génétique Cellulaires, Centre National de la Recherche Scientifique, 118 Route de Narbonne, 31062 Toulouse, France.

[‡]To whom reprint requests should be addressed. E-mail: carlwu@helix.nih.gov.

The publication costs of this article were defrayed in part by page charge payment. This article must therefore be hereby marked “advertisement” in accordance with 18 U.S.C. §1734 solely to indicate this fact.

and assembled as described by Luger *et al.* (40). Aliquots of histone preparations (1 mg/ml) were stored at -80°C .

Histone Acetylation. Recombinant FLAG-p300 was purified from baculovirus-infected SF9 cells as described by Yang *et al.* (41). Recombinant *Drosophila* histone octamers (20 μg) were acetylated in a 250- μl reaction containing 50 mM Tris-HCl, pH 8.0, 10% glycerol, 0.1 mM EDTA, 1 mM DTT, 3 nM at 50 nCi/ μl of [^3H] acetyl-CoA (Amersham Pharmacia), and 1.2 pmol of purified recombinant FLAG-p300. The mixture was incubated at 30°C for 1 h.

Nucleosome Reconstitution and Mobilization. Mononucleosomes were assembled on linear DNA according to the “salt jump” method (42). Carrier DNA (supercoiled plasmid DNA containing the inserted fragment) was mixed with the ^{32}P -labeled DNA (20,000–100,000 cpm, final DNA concentration, 200 $\mu\text{g}/\text{ml}$). The suitable amount of histones (histone/DNA, weight ratio $r_w = 0.6$), in 2 M NaCl/10 mM Tris-HCl (pH 7.5)/100 $\mu\text{g}/\text{ml}$ BSA were added. The mixture was first incubated for 10 min at 37°C , diluted to 50 $\mu\text{g}/\text{ml}$ DNA and 0.5 M NaCl, incubated at the same temperature for 30 min, and finally dialyzed at 4°C against 10 mM Tris-HCl (pH 7.5)/1 mM EDTA for at least 2 h. A histone/DNA weight ratio of 0.6 gave optimal reconstitution of mononucleosomes with little formation of dinucleosomes, as judged by glycerol gradient centrifugation. For experiments involving quantification of the ATPase activity of NURF, nonradioactive 359-bp DNA fragment was substituted for the carrier plasmid DNA.

Nucleosome mobilization was performed at 37°C for 30 min in Nucleosome Sliding Buffer [10 mM Tris-HCl (pH 7.6)/50 mM NaCl/3 mM MgCl_2 /1 mM β -mercaptoethanol/1 mM ATP] at a nucleosome concentration of ≈ 10 μg DNA equivalent/ml, in the presence of 0.5–2 μl of NURF. The standard reaction volume was 10 μl .

Gel Electrophoresis. Mononucleosomes were electrophoresed at room temperature in 4% polyacrylamide (acrylamide/bisacrylamide, 29:1, wt/wt) slab gels (0.15 cm \times 17 cm \times 18 cm) in TE buffer (Tris-HCl 10 mM/EDTA 1 mM, pH 7.8). Gels were preelectrophoresed for 1 h at 200–250 V and electrophoresed at the same voltage for 3 h with extensive buffer recirculation. Gels were dried and autoradiographed at -80°C .

For native two-dimensional gel analysis, the mixed population of nucleosomes was first fractionated on a native 4% TE gel as above, the gel slice containing the mixed population was directly loaded on the top of a 5% polyacrylamide gel (acrylamide/bisacrylamide 20:1, wt/wt) in TGE buffer (Tris base 25 mM/glycine 190 mM/EDTA 1 mM). Gels were electrophoresed for 4 h at 250 V.

For histone–DNA quantification, the mixed population of nucleosomes was first fractionated on a native gel as above. Nucleosome bands were excised and loaded directly onto the second dimension 15% SDS–polyacrylamide gel. DNA and histones were visualized by silver staining (43).

For the characterization of acetylated isoforms, histones were first separated on a 15% SDS–polyacrylamide gel and visualized by Coomassie blue staining. Histones were excised and incubated in a soaking solution containing acetic acid (1 M), ammonia (0.03 M), and mercaptoethylamine-HCl (1%) for 1 h. The gel slice was then directly loaded on the top of the second dimension and embedded in place with a melted agarose solution (1% in water). The second-dimension gel contained urea (5 M), acrylamide (20%), bis-acrylamide (0.1), acetic acid (1 M), glycine (0.1 M). The running buffer contained acetic acid (1 M), glycine (0.1 M), and cetyltrimethylammonium bromide (0.15%) (44).

Purification of NURF. NURF was purified to the final glycerol gradient step from 200 g of 0–12 h *Drosophila* embryos, as described

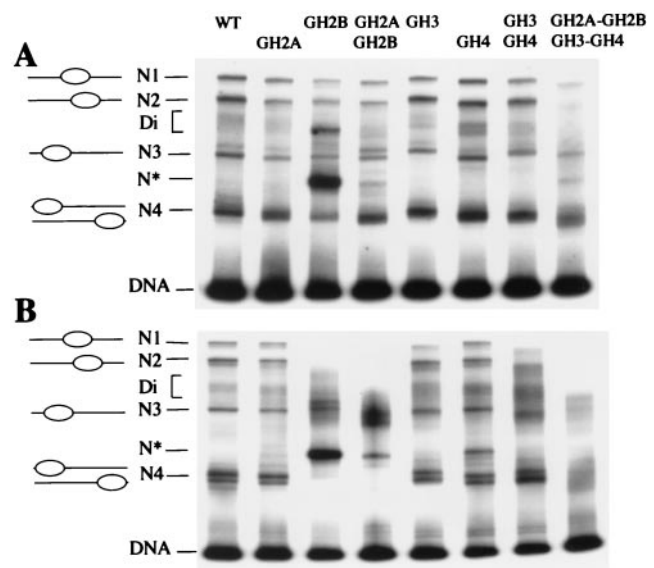


Fig. 1. (A) Influence of histone tails on nucleosome assembly and positioning. Mononucleosomes lacking histone N-terminal tails were reconstituted on a radiolabeled 359-bp *hsp70* promoter fragment and electrophoresed on a 4% native polyacrylamide gel in TE buffer. The four major differentially migrating nucleosome species are indicated: N1, N2, N3, and N4. Di, dinucleosome species, confirmed by sedimentation on glycerol gradients. N* is a reconstitution artifact (see text). (B) Electrophoresis of tailless nucleosomes in TGE buffer, as in A.

(19, 45). The concentration of NURF was determined to be 0.8 ng/ μl ISWI equivalents (29).

ATPase Assays. ATPase assays were performed by using α - ^{32}P -labeled ATP as described by Hamiche *et al.* (29). The standard reaction (5 μl) contained: 10 mM Hepes-KOH, pH 7.6, 50 mM KCl, 0.1 mM EDTA, 2 mM MgCl_2 , 0.5 mM DTT, 7.5% glycerol, 0.01% Nonidet P-40, 30 μM ATP, 5 μCi [α - ^{32}P]ATP (300 Ci/mmol, Amersham Pharmacia), 25 ng of mononucleosomes (DNA weight equivalent), 1.5 ng of NURF (and 350 ng of glutathione S-transferase-H4 tail for the experiment in Fig. 4). Reactions were incubated at 37°C for 30 min. The labeled ADP product of ATP hydrolysis was separated by TLC (polyethyleneimine cellulose on polyester; Sigma) by using 0.75 M KH_2PO_4 (1.0- μl load).

Results

Histone N-Terminal Tails Modulate Nucleosome Positioning. We generated recombinant DNA constructs for bacterial expression of WT and mutant *Drosophila* histones lacking the N-terminal histone tails. The “tailless” histones were constructed by removing sequences corresponding to residues preferentially cleaved from nucleosomal histones by trypsin, leaving behind the histone globular domains (46). We purified bacterially expressed full-length and tailless histones (see Fig. 6, which is published as supporting information on the PNAS web site, www.pnas.org). Mononucleosomes reconstituted from full length recombinant *Drosophila* histones adopt four major positions (N1–N4) on the 359-bp *hsp70* promoter when analyzed by native gel electrophoresis at low ionic strength (TE buffer: 10 mM Tris-Cl, pH 7.8/1 mM EDTA) (Fig. 1A, WT). These nucleosomal locations, which generate distinct electrophoretically separable nucleosome conformations depending on the length of linker DNA extending from each end of the core particle (39, 47), are the same as those reported for nucleosomes reconstituted from native *Drosophila* histones (29). The similar nucleosome positions validate use of bacterially expressed proteins. We found that removal of the histone H2B tail led to the assembly of a highly prominent nucleoprotein species (N*) located between

nucleosomes N3 and N4, and a minor species between N2 and N3 (Fig. 1B; GH2B). Curiously, the intensity of N* is reduced, and the minor species is absent when both H2A and H2B tails were simultaneously removed. As described below, these unusual species are artifacts of reconstitution.

Removal of the N-terminal tail from an individual core histone or from two histones in combination had insignificant effects on the electrophoretic migration of N1–N4 nucleosomes (Fig. 1A). Removal of the histone H3 tail did reveal a slightly slower gel migration for all N1–N4 nucleosome species. By contrast, the combined removal of all four histone tails diminished the N2 nucleosome; in addition, N1, N3, and N4 species were also diminished relative to the heterogenous background signal. Given early indications that increased salt concentrations can disrupt interactions between nucleosomal histones and DNA (48–50), we used an alternative electrophoresis buffer that contains a higher electrolyte concentration (TGE: 25 mM Tris base/190 mM glycine/1 mM EDTA, pH 8.3) to promote destabilization of histone tail interactions with DNA.

On electrophoresis in TGE, nucleosomes lacking the H2B tail alone or the tails of H2A and H2B showed a striking loss of N1, N2, and N4 nucleosomes and a gain in the N3 species (Fig. 1B; GH2B, GH2A–GH2B). These tailless N3 species also showed greater electrophoretic heterogeneity when compared with WT N3. Similar results were observed on electrophoresis of H2B tailless nucleosomes in Tris·borate·EDTA (data not shown). When both H3 and H4 tails were removed, we observed heterogeneous migration and some depletion of N1–N3 nucleosomes (Fig. 1B, GH3–GH4). When all four N-terminal histone tails were removed, we observed complete depletion of the N1 and N2 nucleosomes and greater heterogeneity in migration of N3 and N4. The enhancement of nucleosome mobility in TGE appears to be because of the destabilizing effects of gel electrophoresis as well as the TGE buffer, as it was not observed when nucleosomes were first incubated in TGE before subsequent electrophoresis in TE buffer (data not shown). We conclude that the H2B tail, with additional contributions from the other three histone tails, is important for maintaining the translational positions of histone octamers under assay conditions.

Dynamics of Nucleosome Sliding. We examined the dynamics of nucleosome mobility further by using two-dimensional native gel electrophoresis (47). Mononucleosomes lacking one or more tails were first separated on a native gel in TE, followed by native gel electrophoresis in the second-dimension in TGE. Any movement of nucleosomes on electrophoresis in the second dimension should be evident from the electrophoretic migration of nucleosomes away from the diagonal. We observed little effect on nucleosome dynamics for WT nucleosomes and nucleosomes lacking N-terminal tails of histones H2A, H3, and H4 individually and H3 and H4 tails in combination (Fig. 2). The observed tendency for electrophoretic migration away from the diagonal is: WT < GH2A = GH4 < GH3 < (GH3–GH4). However, removal of the H2B tail alone revealed nucleosomes moving off the diagonal, from one position to another linked together by smeary lines, suggesting that movement was induced slowly during gel electrophoresis (Fig. 2, GH2B). We also found that removal of both H2A and H2B tails resulted in redistribution of nucleosomes to a heterogeneous region around N3 (Fig. 2; GH2A–GH2B); the absence of smears linked to the original positions suggests that nucleosome movement was probably induced quickly at the onset of electrophoresis. Removal of all four histone tails resulted in the induction of even greater nucleosome mobility around N3 (Fig. 2; GH2A–GH2B–GH3–GH4).

Increased Nucleosome Mobility Is Not Caused by Histone Loss. To assess whether the increased dynamics of nucleosomes lacking the H2B N-terminal tail is accompanied by a change in the composition of the histone octamer, we examined the state of nucleosomal

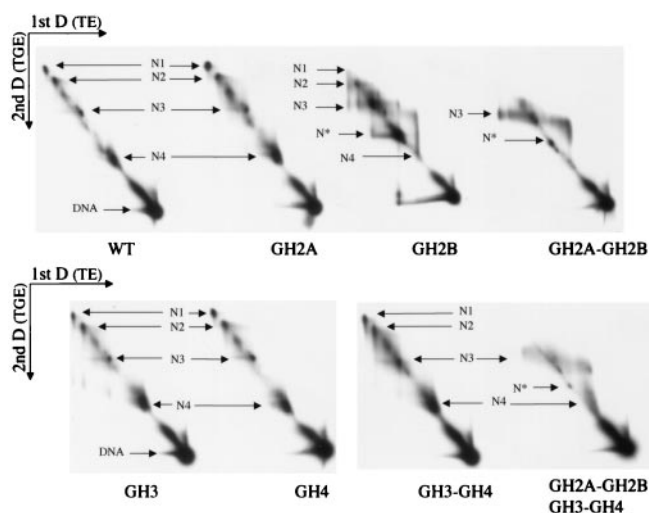


Fig. 2. Two-dimensional native gels showing dynamics of nucleosome sliding. Electrophoresis of 359-bp *hsp70* mononucleosomes containing WT and mutant histones was first conducted in TE buffer (4% polyacrylamide gel). Entire gel lanes containing the separated nucleoprotein species identical to Fig. 1B were excised and applied horizontally for electrophoresis on 5% polyacrylamide gels in TGE buffer. The electrophoretic positions of N1–N4, N*, and free DNA are indicated.

histones after the induction of sliding. Nucleosomes lacking the H2B N-terminal tail that had mobilized to the N3 region (Fig. 3A) were isolated by excision of the gel band and analyzed by SDS/PAGE and silver staining. We found all four core histones present in these nucleosomes (Fig. 3B), showing the integrity of the histone octamer lacking the H2B N-terminal tail after mobilization.

Consistent with these results, H2B tailless nucleosomes showed a glycerol gradient sedimentation profile similar to that of mononucleosomes reconstituted from full length histones (data not shown). We also found that the N* species generated by reconstitution of H2B tailless nucleosomes sedimented between mononucleosomes and free DNA. The N* species was unstable in solution at moderate salt concentrations; incubation of H2B tailless nucleosomes in 100 mM NaCl before native gel electrophoresis in TE buffer greatly reduced its appearance (Fig. 3C). N* could not be isolated as a stable complex after gel elution, thus precluding further analysis by nuclease digestion techniques. We conclude that

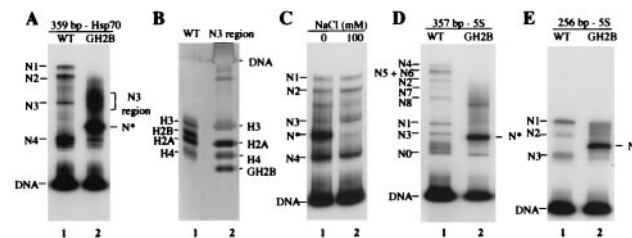


Fig. 3. (A) Characterization of mobilized H2B tailless nucleosome. Mononucleosomes containing WT recombinant histones and lacking histone H2B N-terminal tails (GH2B) were reconstituted on a radiolabeled 359-bp *hsp70* promoter fragment and electrophoresed on a 4% native polyacrylamide in TGE buffer. N* is a reconstitution artifact (see text). (B) Histone composition of GH2B nucleosomes migrating to the N3 region. The corresponding native gel band (A, lane 2) was excised and analyzed by SDS/PAGE and silver staining. (C) N* is greatly reduced in 100 mM NaCl. *hsp70* mononucleosomes (359 bp) lacking histone H2B tails were incubated for 1 h at room temperature in TE buffer containing 100 mM NaCl. The sample was electrophoresed on a 4% native polyacrylamide gel in TE buffer. (D and E) Mononucleosomes containing recombinant histones (WT) or histones lacking H2B N-terminal tails (GH2B) were reconstituted on radiolabeled 357-bp 5S and 256-bp 5S DNA fragments and electrophoresed as above in TGE buffer.

N* is likely to be an artifact of reconstitution, which generates a nucleohistone complex that is not fully folded or assembled in a canonical nucleosome.

H2B Tailless Nucleosomes Are Also Mobile on 5S DNA. To extend the analysis of nucleosome dynamics to DNA sequences other than the *hsp70* promoter, we used DNA fragments from the sea urchin 5S ribosomal DNA gene. Reconstitution of mononucleosomes on 357- and 256-bp 5S DNA fragments with bacterially expressed *Drosophila* histones revealed multiple nucleosome species migrating at positions similar to those previously observed for 5S nucleosomes reconstituted with native (duck) histone octamers (39, 51) (Fig. 3 D and E). When 5S nucleosomes lacking the H2B N-terminal tail were reconstituted and analyzed by native gel electrophoresis in TGE buffer, we observed a dramatic smearing of specific nucleosome bands, showing changes in nucleosome positioning (Fig. 3 D and E, compare lanes 1 and 2). A prominent nucleoprotein species with N* behavior was also generated, indicating that the reconstitution artifact for nucleosomes lacking the H2B N-terminal tail is not unique to *hsp70*.

Histone N-terminal tails undergo extensive posttranslational modifications such as lysine acetylation, which have profound effects on gene transcription *in vivo* and on chromatin architecture *in vitro* (47, 52–54). We examined whether nucleosome mobility could be affected by acetylation of histones with the p300 histone acetyltransferase (55). p300 specifically acetylates all sites of histone H2A and H2B known to be acetylated in bulk chromatin and preferentially acetylates histone H3 lysines 14 and 18, and histone H4 lysines 5 and 8 (41). As a sensitive measure of nucleosome sliding, we used two-dimensional native gel electrophoresis with TE buffer in the first dimension and TGE buffer in the second dimension. We found no evidence of migration away from the diagonal when nucleosomal histones were acetylated (see Fig. 7, which is published as supporting information on the PNAS web site, www.pnas.org).

Importance of Histone H4 Tail for NURF Activity. To examine how the histone N-terminal tails influence NURF-mediated nucleosome sliding, we analyzed the ability of tailless nucleosomes to stimulate the ATPase activity of NURF. Incubation of NURF with nucleosomes lacking histone H2A, H2B, or H3 tails individually or lacking both H2A and H2B tails showed stimulation of ATPase activity like that generated by WT nucleosomes (Fig. 4A). By contrast, nucleosomes lacking the histone H4 tail alone or combined with removal of other histone tails showed no stimulation of the ATPase activity of NURF (Fig. 4A).

We investigated the effects of tailless nucleosomes on nucleosome sliding by NURF (Fig. 4B). For WT nucleosomes and nucleosomes lacking the histone H2A, H2B, or H3 tail, we observed NURF-mediated nucleosome mobility similar to that reported for nucleosomes containing native full length histones (29) (Fig. 4B; WT, GH2A, GH2B, and GH3). Nucleosomes N1 and N2 were depleted, whereas N3 was enriched, along with slower migration of the N4 “fragment end nucleosomes” (the N* species was not mobilized by NURF). In contrast, nucleosomes lacking the H4 tail showed little mobilization on reaction with NURF (Fig. 4B; GH4). N1 and N2 positions were retained, whereas N3 showed little enrichment (but the N4 nucleosomes showed clear changes in migration). Taken together, the results demonstrate that the N-terminal tail of histone H4 regulates the activity of NURF.

We examined whether a glutathione *S*-transferase (GST)-histone H4 tail fusion could block nucleosome stimulation of the ATPase activity of NURF *in trans*. Consistent with previous work (36), GST-H4 tail reduced stimulation of the ATPase activity of NURF by only 2-fold when introduced at 100-fold molar excess to nucleosomes (Fig. 4A, lane 13). The ability of NURF to catalyze nucleosome sliding was not detectably affected by a 100-fold molar excess of GST-H4 tail (Fig. 4B), and higher concentrations of GST-H4 tail

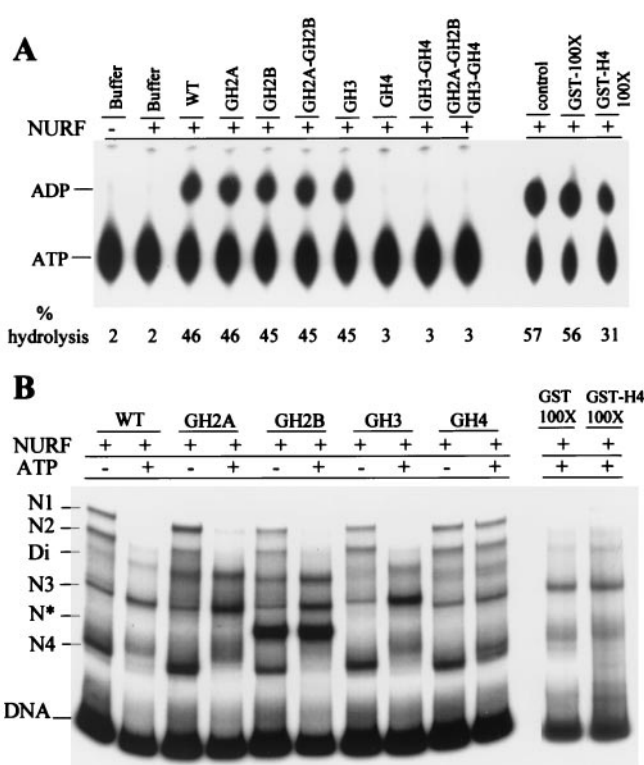


Fig. 4. Requirement of histone H4 N-terminal tail for NURF activity. (A) Stimulation of ATPase activity of NURF by nucleosomes. ATPase assays contained WT nucleosomes or nucleosomes lacking histone tails, as indicated. ATPase activity was measured by hydrolysis of [α - 32 P]ATP to [α - 32 P]ADP and visualized by TLC. ATPase assays were conducted in the presence of GST or GST-H4 tail proteins, as indicated. (B) Nucleosome sliding assay. *hsp70* mononucleosomes (359 bp) reconstituted from WT or mutant histones were incubated with NURF in the presence or absence of ATP and electrophoresed (4% polyacrylamide gel) in TE buffer. WT mononucleosomes were reacted with NURF and ATP in the presence of GST or GST-H4 tail proteins, as indicated, before electrophoresis.

failed to show inhibition (data not shown). It appears that the H4 tail is unable to influence NURF-induced nucleosome sliding when removed from the context of the nucleosome.

Histone H4 Residues 16-KRHR-19 Constitute a Regulatory Motif. To further define histone H4 residues important for regulating the activity of NURF, we conducted alanine scanning mutagenesis of the histone H4 tail. We introduced alanine substitutions in histone H4 residues 9–11 [H4 (9–11)A], residues 13–14 [H4 (13, 14)A], and residues 16–19 [H4 (16–19)A]. We purified bacterially expressed mutant proteins and reconstituted each of the H4 tail mutants with the remaining, WT core histones (Fig. 5A). (Mutagenesis of histone H4 residues 1–8, which are essentially identical to the corresponding residues of histone H2A, was not conducted.) Nucleosome mobility similar to the sliding induced on WT nucleosomes was observed for nucleosomes bearing H4 (9–11)A and H4 (13, 14)A (Fig. 5B; N3/N1 ratios 35.0, 28.5). However, the sliding of nucleosomes containing H4 (16–19)A was significantly reduced to the level displayed for H4 tailless nucleosomes (GH4) (Fig. 5B; N3/N1 ratios 5.5 vs. 4.7). The results demonstrate that histone H4 residues 16-KRHR-19 are critical for activating NURF. Finally, hybrid nucleosomes in which the N-terminal tails of histone H3 and H4 were exchanged showed significant reduction of ATP-dependent nucleosome mobility compared with that of WT nucleosomes (Fig. 5B; H3t-GH4, H4t-GH3: N3/N1 ratio 6.2 vs. 34.4). Hence, the location of the histone H4 tail motif 16-KRHR-19 relative to the nucleosome core particle is functionally important. The influence

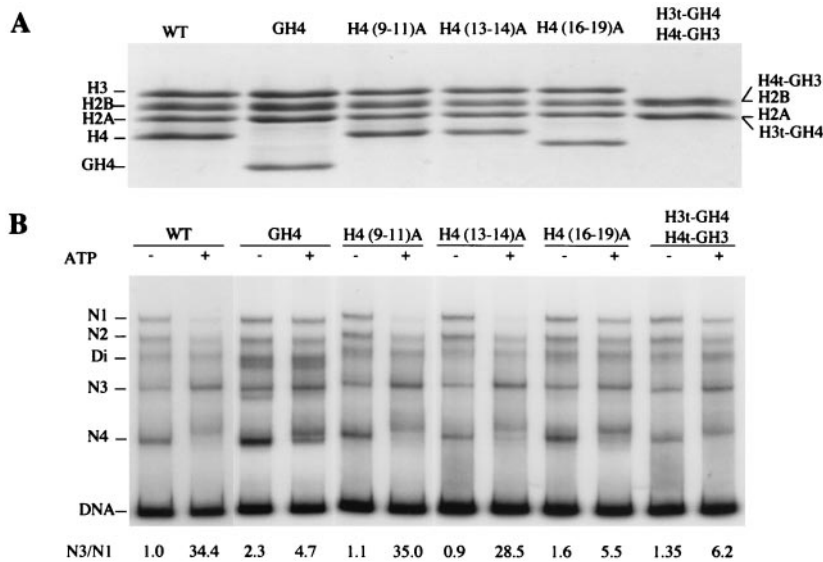


Fig. 5. (A) Alanine scanning mutagenesis of the histone H4 tail and exchange of the H3 and H4 tails. SDS/PAGE (15% polyacrylamide) and Coomassie blue staining of histone octamers assembled from purified WT and mutant histones, as indicated. A, alanine; t, tail; G, globular domain. (B) Importance of histone H4 residues 16-KRHR-19 for NURF-mediated nucleosome sliding. *hsp70* mononucleosomes (359 bp) reconstituted from WT or mutant histones, as indicated, were incubated with NURF in the presence or absence of ATP, electrophoresed on a 4% native polyacrylamide gel in TE buffer, and visualized by autoradiography.

of histone H4 tail mutations on nucleosome sliding is corroborated by similar effects on the ATPase activity of NURF (see Fig. 8, which is published as supporting information on the PNAS web site, www.pnas.org).

Discussion

The x-ray crystal structure of the nucleosome core particle shows that the N-terminal tails of histones H3 and H2B exit through the aligned minor grooves of adjacent gyres of the DNA superhelix, whereas H4 and H2A tails exit in minor grooves from the top or bottom edges of the disk-like particle (56). Beyond the nucleosome core particle, the histone tails are disordered, having no visible interactions with the 147-bp DNA superhelix (56). Biophysical studies of nucleosome arrays in which the histone tails are removed by trypsinization or modified by acetylation indicate their involvement in the higher-order folding of chromatin (57–65). Moreover, contacts can be observed between the tails and the histone octamer of neighboring core particles in the x-ray crystal structure (56).

However, there is evidence that the N-terminal histone tails also interact with core particle DNA in solution. The absence of histone N-terminal tails decreases the thermostability of the nucleosome (66) and alters the equilibrium constants for dynamic DNA site accessibility in nucleosomes (67). Binding of sequence-specific transcription factors to the nucleosome is modulated by the presence of the histone tails (68–71), and photochemical and UV-laser crosslinking experiments reveal physical interactions between core histone tails and nucleosomal DNA (50, 72). The histone tails not only make contact with DNA in the nucleosome core particle but also can preferentially interact with linker DNA (73). Stabilization of nucleosomes by histone tails is apparently effective only on intrinsically straight or bent, rather than flexible, DNA fragments (74).

Our study provides an additional perspective for the histone N-terminal tails. We found that deletion of the N-terminal tail of histone H2B promoted uncatalyzed nucleosome mobility when perturbed by native gel electrophoresis in Tris-glycine-EDTA (or Tris-borate-EDTA), and that this effect was increased by deletion of the other histone tails. The observed changes in electrophoretic migration are likely to be caused by increased translational mobility of the histone octamer on DNA, although the additional possibility of increased conformational flexibility of the linker DNA is not excluded. Thus, uncatalyzed nucleosome positioning and mobility not only may depend on structured histone–DNA interactions in the nucleosome core particle but also could be modulated by

interactions of the histone H2B tail and other histone tails with nucleosomal DNA. The proximity of the basic histone H2B tails to two adjacent DNA gyres of the nucleosome core particle may provide especially suitable interactions that restrict nucleosome mobility. In this respect, it is intriguing to recall genetic studies in which deletion of the first 20 amino acids of the H2B N-terminal tail bypassed the requirement for Swi-Snf in yeast (75).

It is of interest that quantitative hyperacetylation of core histones by p300 had no detectable effect on nucleosome positioning or nucleosome dynamics. These results, which suggest that histone acetylation by p300 has a significantly greater impact on higher-order folding of nucleosome arrays than on the positioning and mobility (or stability) of individual nucleosomes, concur with other findings of a similar nature (74, 76, 77). We also note parenthetically that deletion of the histone H3 tail produced a slight retardation in electrophoretic migration irrespective of nucleosome positioning, raising the possibility that this histone tail affects the entry–exit angle of the linker DNA.

We demonstrated the importance of the histone H4 tail in ATP-dependent nucleosome sliding catalyzed by NURF. This finding concurs with results showing that the histone H4 tail is required for induction of nucleosome sliding by the CHRAC chromatin remodeling complex and for stimulation of the ATPase activity of recombinant ISWI (78). Given that ISWI is a common component of NURF and CHRAC, it is likely that interactions between the H4 tail and ISWI are important for activating NURF. Full efficiency and positional specificity of nucleosome sliding require the participation of the largest NURF subunit, NURF301 (79).

The definition by alanine-scanning mutagenesis of histone H4 tail residues responsible for regulating NURF activity reveals that H4 16-KRHR-19 are critical for the induction of ATP-dependent nucleosome sliding. The proper spatial location of this regulatory motif relative to the global structure of the nucleosome is also important, because interchanging the tails of H3 and H4 impaired nucleosome sliding by NURF. These findings, taken with the failure of a GST-H4 tail fusion protein to significantly inhibit NURF function, suggest that NURF probably interacts with H4 tail residues 16-KRHR-19 in complex with nucleosomal DNA. There is evidence that part of the N-terminal tails of histone H4 (and H3) can be organized in the nucleosome as DNA-bound polypeptide segments with α -helical character (80). It will be interesting to investigate the nature of the regulatory interaction between H4 16-KRHR-19 and NURF (ISWI). Given that H4 K16 and K20 are

known sites of histone acetylation and methylation, respectively, it is possible that these modifications could influence the activities of NURF and other ISWI complexes.

Aside from the evident importance of histone H4 16-KRHR-19 in providing a key to the ATP-dependent catalytic activity of NURF, the involvement of the other core histone tails in catalyzed nucleosome sliding is unclear. Deletion of the histone H2B tail did not bypass the need for NURF to induce ATP-dependent nucleosome sliding under *in vitro* assay conditions, indicating that DNA-protein interactions within the nucleosome core particle are dominant. An attractive model for nucleosome sliding invokes the ATP-dependent induction and propagation of a DNA twist or bulge over the histone octamer, a process that necessitates the

transient disruption of contacts between structured histone elements and core particle DNA (29–31, 81, 82). However, it is possible that the dissociation of the N-terminal tail of histone H2B and the other histone tails from nucleosomal DNA may facilitate the overall nucleosome sliding mechanism.

We thank members of our laboratory for helpful comments and discussion, Y. Nakatani (Dana-Farber Cancer Center) for the recombinant p300 histone acetyltransferase baculovirus, and R. Sandaltzopoulos (National Institutes of Health) for a NURF sample. A.H. was supported by a fellowship from the Human Frontiers of Science Program and J.G.K. by a National Institutes of Health Visiting Fellowship. This work was supported by the Intramural Research Program of the National Cancer Institute, USA, and by l'Association pour la Recherche sur le Cancer, France.

1. Van Holde, K. E. (1989) *Chromatin* (Springer, New York).
2. Elgin, S. C. (1990) *Curr. Opin. Cell Biol.* **2**, 437–445.
3. Kornberg, R. D. & Lorch, Y. (1999) *Cell* **98**, 285–294.
4. Wu, J. & Grunstein, M. (2000) *Trends Biochem. Sci.* **25**, 619–623.
5. Vignali, M., Hassan, A. H., Neely, K. E. & Workman, J. L. (2000) *Mol. Cell. Biol.* **20**, 1899–1910.
6. Eisen, A. & Lucchesi, J. C. (1998) *BioEssays* **20**, 634–641.
7. Guschin, D. & Wolffe, A. P. (1999) *Curr. Biol.* **9**, R742–R746.
8. Peterson, C. L. (2000) *FEBS Lett.* **476**, 68–72.
9. Armstrong, J. A., Bieker, J. J. & Emerson, B. M. (1998) *Cell* **95**, 93–104.
10. Kadonaga, J. T. (1998) *Cell* **92**, 307–313.
11. Workman, J. L. & Kingston, R. E. (1998) *Annu. Rev. Biochem.* **67**, 545–579.
12. Muchardt, C. & Yaniv, M. (1999) *Semin. Cell Dev. Biol.* **10**, 189–195.
13. Sudarsanam, P., Iyer, V. R., Brown, P. O. & Winston, F. (2000) *Proc. Natl. Acad. Sci. USA* **97**, 3364–3369. (First Published March 21, 2000; 10.1073/pnas.050407197)
14. Kingston, R. E. & Narlikar, G. J. (1999) *Genes Dev.* **13**, 2339–2352.
15. Goldmark, J. P., Fazio, T. G., Estep, P. W., Church, G. M. & Tsukiyama, T. (2000) *Cell* **103**, 423–433.
16. Deuring, R., Fantì, L., Armstrong, J. A., Sarte, M., Papoulas, O., Prestel, M., Daubresse, G., Verardo, M., Moseley, S. L., Berloco, M., et al. (2000) *Mol. Cell.* **5**, 355–365.
17. Kikyo, N., Wade, P. A., Guschin, D., Ge, H. & Wolffe, A. P. (2000) *Science* **289**, 2360–2362.
18. Shen, X., Mizuguchi, G., Hamiche, A. & Wu, C. (2000) *Nature (London)* **406**, 541–544.
19. Tsukiyama, T. & Wu, C. (1995) *Cell* **83**, 1011–1020.
20. Tsukiyama, T., Daniel, C., Tamkun, J. & Wu, C. (1995) *Cell* **83**, 1021–1026.
21. Ito, T., Bulger, M., Pazin, M. J., Kobayashi, R. & Kadonaga, J. T. (1997) *Cell* **90**, 145–155.
22. Varga-Weisz, P. D., Wilms, M., Bonte, E., Dumas, K., Mann, M. & Becker, P. B. (1997) *Nature (London)* **388**, 598–602.
23. LeRoy, G., Orphanides, G., Lane, W. S. & Reinberg, D. (1998) *Science* **282**, 1900–1904.
24. Tsukiyama, T., Palmer, J., Landel, C. C., Shiloach, J. & Wu, C. (1999) *Genes Dev.* **13**, 686–697.
25. Bochar, D. A., Savard, J., Wang, W., Lafleur, D. W., Moore, P., Cote, J. & Shiekhattar, R. (2000) *Proc. Natl. Acad. Sci. USA* **97**, 1038–1043.
26. LeRoy, G., Loyola, A., Lane, W. S. & Reinberg, D. (2000) *J. Biol. Chem.* **275**, 14787–14790.
27. Poot, R. A., Deldaire, G., Hulsman, B. B., Grimaldi, M. A., Corona, D. F., Becker, P. B., Bickmore, W. A. & Varga-Weisz, P. D. (2000) *EMBO J.* **19**, 3377–3387.
28. Guschin, D., Geiman, T. M., Kikyo, N., Tremethick, D. J., Wolffe, A. P. & Wade, P. A. (2000) *J. Biol. Chem.* **275**, 35248–35255.
29. Hamiche, A., Sandaltzopoulos, R., Gdula, D. A. & Wu, C. (1999) *Cell* **97**, 833–842.
30. Langst, G., Bonte, E. J., Corona, D. F. & Becker, P. B. (1999) *Cell* **97**, 843–852.
31. Whitehouse, I., Flaus, A., Cairns, B. R., White, M. F., Workman, J. L. & Owen-Hughes, T. (1999) *Nature (London)* **400**, 784–787.
32. Cote, J., Peterson, C. L. & Workman, J. L. (1998) *Proc. Natl. Acad. Sci. USA* **95**, 4947–4952.
33. Schnitzler, G., Sif, S. & Kingston, R. E. (1998) *Cell* **94**, 17–27.
34. Bazett-Jones, D. P., Cote, J., Landel, C. C., Peterson, C. L. & Workman, J. L. (1999) *Mol. Cell. Biol.* **19**, 1470–1478.
35. Lorch, Y., Zhang, M. & Kornberg, R. D. (1999) *Cell* **96**, 389–392.
36. Georgel, P. T., Tsukiyama, T. & Wu, C. (1997) *EMBO J.* **16**, 4717–4726.
37. Simpson, R. T. & Stafford, D. W. (1983) *Proc. Natl. Acad. Sci. USA* **80**, 51–55.
38. Simpson, R. T., Thoma, F. & Brubaker, J. M. (1985) *Cell* **42**, 799–808.
39. Duband-Goulet, I., Carot, V., Ulyanov, A. V., Douc-Rasy, S. & Prunell, A. (1992) *J. Mol. Biol.* **224**, 981–1001.
40. Luger, K., Rechsteiner, T. J., Flaus, A. J., Waye, M. M. & Richmond, T. J. (1997) *J. Mol. Biol.* **272**, 301–311.
41. Yang, X. J., Ogryzko, V. V., Nishikawa, J., Howard, B. H. & Nakatani, Y. (1996) *Nature (London)* **382**, 319–324.
42. Stein, A. (1979) *J. Mol. Biol.* **130**, 103–134.
43. Wray, W., Boulikas, T., Wray, V. P. & Hancock, R. (1981) *Anal. Biochem.* **118**, 197–203.
44. Rogakou, E. P., Redon, C., Boon, C., Johnson, K. & Bonner, W. M. (2000) *BioTechniques* **28**, 38–40, 42, 46.
45. Sandaltzopoulos, R., Ossipow, V., Gdula, D. A., Tsukiyama, T. & Wu, C. (1999) *Methods Enzymol.* **304**, 757–765.
46. Bohm, L. & Crane-Robinson, C. (1984) *Biosci. Rep.* **4**, 365–386.
47. Meersseman, G., Pennings, S. & Bradbury, E. M. (1992) *EMBO J.* **11**, 2951–2959.
48. Spadafora, C., Oudet, P. & Chambon, P. (1979) *Eur. J. Biochem.* **100**, 225–235.
49. Yager, T. D. & van Holde, K. E. (1984) *J. Biol. Chem.* **259**, 4212–4222.
50. Mutskov, V., Gerber, D., Angelov, D., Ausio, J., Workman, J. & Dimitrov, S. (1998) *Mol. Cell. Biol.* **18**, 6293–6304.
51. Hamiche, A., Schultz, P., Ramakrishnan, V., Oudet, P. & Prunell, A. (1996) *J. Mol. Biol.* **257**, 30–42.
52. Hansen, J. C., Tse, C. & Wolffe, A. P. (1998) *Biochemistry* **37**, 17637–17641.
53. Kuo, M. H. & Allis, C. D. (1998) *BioEssays* **20**, 615–626.
54. Ura, K., Hayes, J. J. & Wolffe, A. P. (1995) *EMBO J.* **14**, 3752–3765.
55. Schiltz, R. L., Mizzen, C. A., Vassilev, A., Cook, R. G., Allis, C. D. & Nakatani, Y. (1999) *J. Biol. Chem.* **274**, 1189–1192.
56. Luger, K., Mader, A. W., Richmond, R. K., Sargent, D. F. & Richmond, T. J. (1997) *Nature (London)* **389**, 251–260.
57. Garcia-Ramirez, M., Dong, F. & Ausio, J. (1992) *J. Biol. Chem.* **267**, 19587–19595.
58. Schwarz, P. M., Felthouser, A., Fletcher, T. M. & Hansen, J. C. (1996) *Biochemistry* **35**, 4009–4015.
59. Tse, C., Sera, T., Wolffe, A. P. & Hansen, J. C. (1998) *Mol. Cell. Biol.* **18**, 4629–4638.
60. Fletcher, T. M. & Hansen, J. C. (1995) *J. Biol. Chem.* **270**, 25359–25362.
61. Garcia-Ramirez, M., Rocchini, C. & Ausio, J. (1995) *J. Biol. Chem.* **270**, 17923–17928.
62. Moore, S. C. & Ausio, J. (1997) *Biochem. Biophys. Res. Commun.* **230**, 136–139.
63. Tse, C. & Hansen, J. C. (1997) *Biochemistry* **36**, 11381–11388.
64. Carruthers, L. M. & Hansen, J. C. (2000) *J. Biol. Chem.* **275**, 37285–37290.
65. Wang, X., He, C., Moore, S. C. & Ausio, J. (2001) *J. Biol. Chem.* **276**, 12764–12768.
66. Ausio, J., Dong, F. & van Holde, K. E. (1989) *J. Mol. Biol.* **206**, 451–463.
67. Polach, K. J., Lowary, P. T. & Widom, J. (2000) *J. Mol. Biol.* **298**, 211–223.
68. Lee, D. Y., Hayes, J. J., Pruss, D. & Wolffe, A. P. (1993) *Cell* **72**, 73–84.
69. Godde, J. S., Nakatani, Y. & Wolffe, A. P. (1995) *Nucleic Acids Res.* **23**, 4557–4564.
70. Vettese-Dadey, M., Grant, P. A., Hebbes, T. R., Crane-Robinson, C., Allis, C. D. & Workman, J. L. (1996) *EMBO J.* **15**, 2508–2518.
71. Vitolo, J. M., Thiriet, C. & Hayes, J. J. (2000) *Mol. Cell. Biol.* **20**, 2167–2175.
72. Lee, K. M. & Hayes, J. J. (1997) *Proc. Natl. Acad. Sci. USA* **94**, 8959–8964.
73. Angelov, D., Vitolo, J. M., Mutskov, V., Dimitrov, S. & Hayes, J. J. (2001) *Proc. Natl. Acad. Sci. USA* **98**, 6599–6604. (First Published May 29, 2001; 10.1073/pnas.121171498)
74. Widlund, H. R., Vitolo, J. M., Thiriet, C. & Hayes, J. J. (2000) *Biochemistry* **39**, 3835–3841.
75. Recht, J. & Osley, M. A. (1999) *EMBO J.* **18**, 229–240.
76. Mizuguchi, G., Vassilev, A., Tsukiyama, T., Nakatani, Y. & Wu, C. (2001) *J. Biol. Chem.* **276**, 14773–14783.
77. Anderson, J. D., Lowary, P. T. & Widom, J. (2001) *J. Mol. Biol.* **307**, 977–985.
78. Clapier, C. R., Langst, G., Corona, D. F., Becker, P. B. & Nightingale, K. P. (2001) *Mol. Cell. Biol.* **21**, 875–883.
79. Xiao, H., Sandaltzopoulos, R., Wang, H. M., Hamiche, A., Ranallo, R., Lee, K. Y., Fu, D. & Wu, C. (2001) *Mol. Cell* **8**, 531–543.
80. Baneres, J. L., Martin, A. & Parello, J. (1997) *J. Mol. Biol.* **273**, 503–508.
81. Havas, K., Flaus, A., Phelan, M., Kingston, R., Wade, P. A., Lilley, D. M. & Owen-Hughes, T. (2000) *Cell* **103**, 1133–1142.
82. Gavin, I., Horn, P. J. & Peterson, C. L. (2001) *Mol. Cell* **7**, 97–104.